

**Proton-Coupled Electron Transfer between 4-Cyanophenol
and Photoexcited Rhenium(I) Complexes with Different
Protonatable Sites**

Journal:	<i>Inorganic Chemistry</i>
Manuscript ID:	ic-2012-00834c.R2
Manuscript Type:	Article
Date Submitted by the Author:	29-Jun-2012
Complete List of Authors:	Bronner, Catherine; Georg-August-University Göttingen, Institute of Inorganic Chemistry Wenger, Oliver; University of Goettingen, Institute of Inorganic Chemistry

SCHOLARONE™
Manuscripts

1
2
3
4
5
6
7
8
9
10
11
12
13
14
15
16
17
18
19
20
21
22
23
24
25
26
27
28
29
30
31
32
33
34
35
36
37
38
39
40
41
42
43
44
45
46
47
48
49
50
51
52
53
54
55
56
57
58
59
60

Proton-Coupled Electron Transfer between 4-Cyanophenol and Photoexcited Rhenium(I) Complexes with Different Protonatable Sites

*Catherine Bronner and Oliver S. Wenger**

Georg-August-Universität, Institut für Anorganische Chemie, Tammannstrasse 4, D-37077 Göttingen,
Germany

oliver.wenger@chemie.uni-goettingen.de

RECEIVED DATE (to be automatically inserted after your manuscript is accepted if required according to the journal that you are submitting your paper to)

ABSTRACT

Two rhenium(I) tricarbonyl diimine complexes, one of them with a 2,2'-bipyrazine (bpz) and a pyridine (py) ligand in addition to the carbonyls ($[\text{Re}(\text{bpz})(\text{CO})_3(\text{py})]^+$), and one tricarbonyl complex with a 2,2'-bipyridine (bpy) and a 1,4-pyrazine (pz) ligand ($[\text{Re}(\text{bpy})(\text{CO})_3(\text{pz})]^+$) were synthesized and their photochemistry with 4-cyanophenol in acetonitrile solution was explored. Metal-to-ligand charge transfer (MLCT) excitation occurs towards the protonatable bpz ligand in the $[\text{Re}(\text{bpz})(\text{CO})_3(\text{py})]^+$ complex while in the $[\text{Re}(\text{bpy})(\text{CO})_3(\text{pz})]^+$ complex the same type of excitation promotes an electron away from the protonatable pz ligand. This study aimed to explore how this difference in electronic

1 excited-state structure affects the rates and the reaction mechanism for photoinduced proton-coupled
2 electron transfer (PCET) between 4-cyanophenol and the two rhenium(I) complexes. Transient
3 absorption spectroscopy provides clear evidence for PCET reaction products, and significant H/D
4 kinetic isotope effects are observed in some of the luminescence quenching experiments. Concerted
5 proton-electron transfer is likely to play an important role in both cases, but a reaction sequence of
6 proton transfer and electron transfer steps cannot be fully excluded for the 4-cyanophenol /
7 [Re(bpz)(CO)₃(py)]⁺ reaction couple. Interestingly, the rate constants for bimolecular excited-state
8 quenching are on the same order of magnitude for both rhenium(I) complexes.
9
10
11
12
13
14
15
16
17
18
19
20
21
22

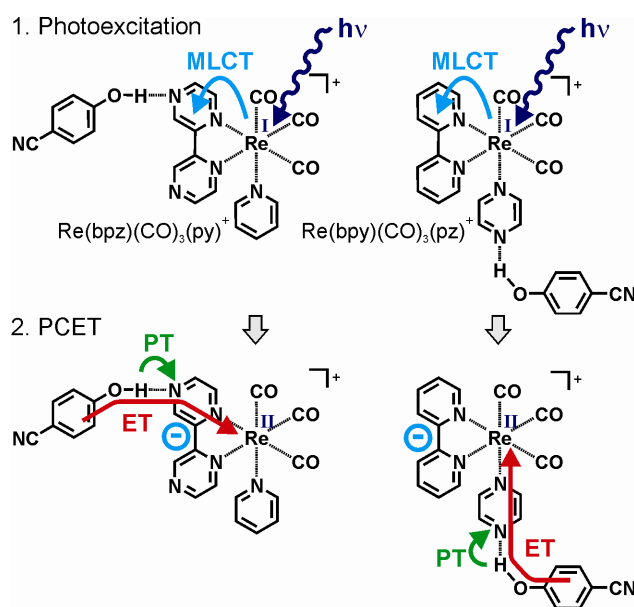
23 INTRODUCTION

24
25
26
27 In view of the importance of proton-coupled electron transfer (PCET) in photosynthesis,¹⁻³
28 respiration,⁴ nitrogen or carbon dioxide fixation⁵ there have been numerous investigations exploring the
29 fundamentals of PCET in recent years.⁶⁻¹⁰ Phenols have played a prominent role in such studies,¹¹⁻¹⁶
30 partly because phenolic functions occur in biologically relevant PCET systems but also because they are
31 simple enough for mechanistic investigations in purely artificial systems. A question of central interest
32 in such studies is often whether the electron and the proton are transferred in a concerted manner or
33 whether there are individual (consecutive) steps of electron transfer and proton transfer.¹⁷⁻¹⁸ A variety of
34 different experimental techniques have been employed including electrochemical,^{10,15} EPR,¹⁹ and optical
35 spectroscopic methods.²⁰⁻²¹
36
37
38
39
40
41
42
43
44
45
46
47

48 Many experimental investigations performed until now focus on PCET between molecules in their
49 electronic ground states, but recently there has been increasing interest in PCET reactivity of
50 photoexcited molecules or metal complexes.²²⁻³³ Such investigations appear interesting in the context of
51 direct light-to-chemical energy conversion, but much is yet to be learned about PCET involving
52 electronically excited states.²⁸
53
54
55
56
57
58
59
60

Against this background we have conducted a comparative study of the excited-state PCET chemistry of the two rhenium(I) tricarbonyl diimine complexes shown in Scheme 1 with 4-cyanophenol as a common reaction partner. Rhenium complexes of this type have long been known as luminophors and photooxidants,³⁴⁻³⁷ and they were frequently employed as sensitizers for photoinduced electron transfer.³⁸⁻⁴⁴ Both complexes from Scheme 1 have protonatable nitrogen atoms at the ligand periphery, either at a 2,2'-bipyrazine (bpz) chelating agent (left) or at a monodentate 1,4-pyrazine (pz) ligand (right). Based on prior studies of photoexcited ruthenium(II) 2,2'-bipyrazine complexes with phenols as reaction partners we anticipated that photoexcitation of the two rhenium complexes from Scheme 1 would induce PCET chemistry when 4-cyanophenol is present at sufficiently high concentration.^{25,28-29,33} Based on these prior investigations we pictured that in aprotic solvent 4-cyanophenol might form hydrogen bonds to the bpz ligand of $[\text{Re}(\text{bpz})(\text{CO})_3(\text{py})]^+$ (py = pyridine) and to the pz ligand of $[\text{Re}(\text{bpy})(\text{CO})_3(\text{pz})]^+$ (bpy = 2,2'-bipyridine), and such encounter adducts would appear to be reasonable precursors for PCET events.

Scheme 1. MLCT excitation and PCET chemistry in two distinct 4-cyanophenol / rhenium reaction couples. ET = electron transfer, PT = proton transfer.



1 The long-lived $^3\text{MLCT}$ (metal-to-ligand charge transfer) state which is populated after photoexcitation
2 is localized on the bidentate bpz and bpy ligands (upper half of Scheme 1). Consequently, MLCT
3 excitation of $[\text{Re}(\text{bpz})(\text{CO})_3(\text{py})]^+$ is expected to increase the basicity of the nitrogen atoms at the
4 periphery of the bpz ligand relative to the ground state (which is beneficial for proton transfer), but at
5 the same time the MLCT-excited electron is in the middle of the electron transfer pathway between 4-
6 cyanophenol and the metal center (lower left corner of Scheme 1). By contrast, MLCT excitation of
7 $[\text{Re}(\text{bpy})(\text{CO})_3(\text{pz})]^+$ opens a direct electron transfer pathway from the phenol to the metal center (lower
8 right corner of Scheme 1), but MLCT excitation in this case is expected to decrease the basicity of the
9 uncoordinated pz nitrogen atom relative to the ground state. We deemed it interesting to explore to what
10 extent, if at all, these two fundamentally different scenarios affect the photoinduced chemistry of 4-
11 cyanophenol / rhenium reaction couples.
12
13
14
15
16
17
18
19
20
21
22
23
24
25
26
27

28 RESULTS AND DISCUSSION

29
30
31
32
33 **X-ray crystal structures.** Yellow monocrystals of $[\text{Re}(\text{bpz})(\text{CO})_3(\text{py})](\text{PF}_6)$ were grown by slow
34 diffusion of pentane into an acetone solution. This compound crystallizes in the monoclinic $\text{C}2/c$ space
35 group with two molecules of the complex and two hexafluorophosphate counter ions in the asymmetric
36 unit. The $[\text{Re}(\text{bpz})(\text{CO})_3(\text{py})]^+$ cation is depicted in Figure 1a (note that only one crystallographically
37 independent cation is represented). A solvate of this structure has already been described by Rillema *et*
38 *al.*⁴⁵
39
40
41
42
43
44
45
46
47

48 The $[\text{Re}(\text{bpy})(\text{CO})_3(\text{pz})]^+$ complex (Figure 1b) was crystallized as the hexafluorophosphate salt by
49 slow evaporation of acetone in an acetone/water mixture at 0°C , affording yellow plates of
50 $[\text{Re}(\text{bpy})(\text{CO})_3(\text{pz})]_2(\text{PF}_6)_2 \cdot (\text{H}_2\text{O}) \cdot ((\text{CH}_3)_2\text{CO})$. The complex crystallizes in the monoclinic $\text{C}2/c$ space
51 group with one rhenium(I) complex and one PF_6^- ion in the asymmetric unit. In addition, a disordered
52 acetone solvent molecule and a water molecule are present, the latter being located on a $\text{C}2$ axis.
53
54
55
56
57
58
59
60

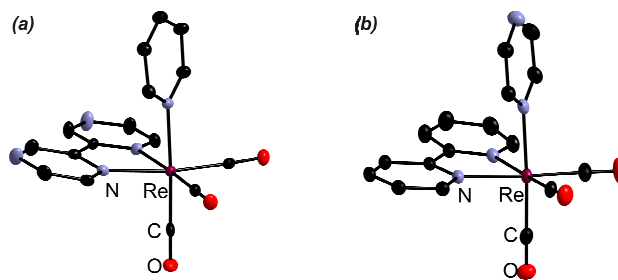


Figure 1. Crystal structures of the $[\text{Re}(\text{bpz})(\text{CO})_3(\text{py})]^+$ (a) and $[\text{Re}(\text{bpy})(\text{CO})_3(\text{pz})]^+$ (b) cations as found in $[\text{Re}(\text{bpz})(\text{CO})_3(\text{py})](\text{PF}_6)$ and $[\text{Re}(\text{bpy})(\text{CO})_3(\text{pz})]_2(\text{PF}_6)_2 \cdot (\text{H}_2\text{O}) \cdot ((\text{CH}_3)_2\text{CO})$, respectively. Thermal ellipsoids are depicted at the 50 % probability level. Hydrogen atoms are omitted for clarity.

In both structures, the rhenium center has its three carbonyl ligands arranged to form the fac-isomer, as is commonly the case for this class of complexes. The coordination sphere is completed by a chelating bpz or bpy ligand and a monodentate py or pz ligand to form an octahedral coordination polyhedron with ligand-metal-ligand angles ranging from 74.84° to 99.18° . The Re-N bond distances are shorter for the chelating bpz and bpy agents than for the monodentate py and pz ligands (Table 1), indicating that the bidentate ligands are bound more strongly to the metal than the monodentate ligands, as is expected.⁴⁶ All Re-C bonds are almost of equal length, showing no elongation in any position (an averaged distance is given in Table 1).

Table 1. Selected average bond distances (in units of Å).

	Re-N _{bpy}	Re-N _{bpz}	Re-N _{py}	Re-N _{pz}	Re-C
$[\text{Re}(\text{bpz})(\text{CO})_3(\text{py})]^+$	-	2.167	2.204	-	1.924
$[\text{Re}(\text{bpy})(\text{CO})_3(\text{pz})]^+$	2.169	-	-	2.209	1.924

[Re(bpy)(CO)₃(pz)]⁺ luminescence quenching. The optical absorption, luminescence, and electrochemical properties of [Re(bpz)(CO)₃(py)]⁺ and [Re(bpy)(CO)₃(pz)]⁺ have been previously explored.^{45,47-50} Both complexes are emissive from ³MLCT states in CH₃CN at room temperature, albeit with significantly different lifetimes (τ): In aerated CH₃CN at 25°C $\tau = 182$ ns for [Re(bpy)(CO)₃(pz)]⁺ while $\tau = 31$ ns for [Re(bpz)(CO)₃(py)]⁺. For the purpose of the present study it was useful to include [Re(bpy)(CO)₃(py)]⁺ as a reference complex with similar electronic structure, but lacking any protonatable sites at the ligand peripheries. This reference complex exhibits a ³MLCT lifetime of 658 ns under the conditions mentioned above.³⁴

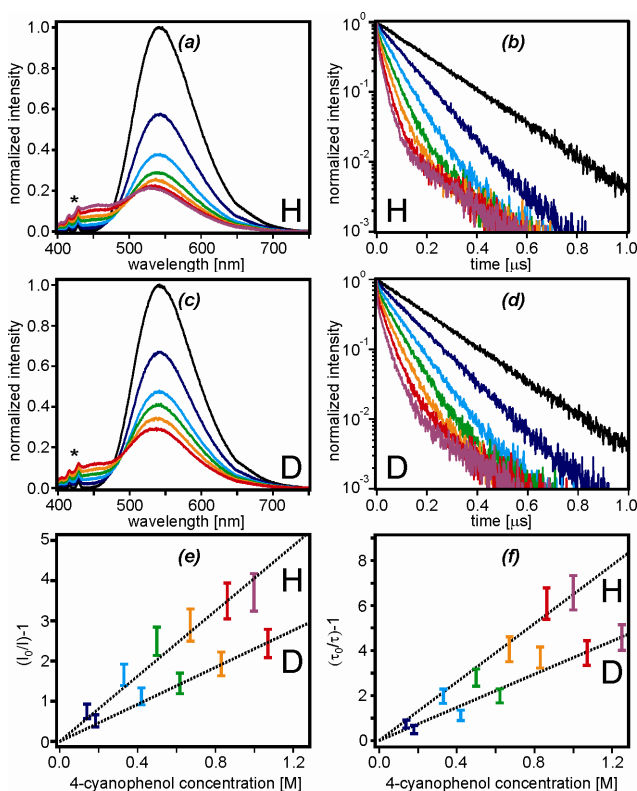


Figure 2. (a, c) Luminescence of [Re(bpy)(CO)₃(pz)]⁺ in CH₃CN in presence of variable amounts of CN-PhOH (a) and CN-PhOD (c) after excitation at 380 nm. (b, d) Luminescence decays of the same complex detected at 542 nm under identical conditions following pulsed excitation at 340 nm. (e, f) Stern-Volmer plots based on the luminescence intensity (e) and lifetime (f) data. A consistent color code was used for all data; the concentrations used for the absorption and emission data in (a) – (d) can be read out from the Stern-Volmer plots in (e) and (f). The y-axes in (a) – (d) are in arbitrary units. The asterisks in (a) and (c) denote Raman scattering peaks.

1
2
3 Figure 2 shows the results of luminescence quenching experiments performed with the
4
5 $[\text{Re}(\text{bpy})(\text{CO})_3(\text{pz})]^+$ complex and 4-cyanophenol (CN-PhOH). The solvent was dried acetonitrile⁵¹
6
7 because 4-cyanophenol concentrations of up to ~1.2 M can easily be achieved in this aprotic solvent.
8
9 The luminescence intensities (Figure 2a) and lifetimes (Figure 2b) are both found to decrease with
10
11 increasing 4-cyanophenol concentration. The luminescence intensity at $\lambda_{\text{max}} = 542$ nm decreases by
12
13 roughly a factor of 5 between solutions containing 0 M and ~1 M 4-cyanophenol, but with increasing 4-
14
15 cyanophenol concentration one detects increasingly intense emission bands in the spectral range
16
17 between 400 nm and 500 nm. These latter bands are also observed from acetonitrile solutions containing
18
19 only 4-cyanophenol (Figure S1 of the Supporting Information; these bands actually have a tail up to
20
21 ~650 nm), and therefore are attributed to emission either from 4-cyanophenol or an emissive impurity
22
23 with which our 4-cyanophenol source is contaminated. The latter assignment makes particular sense
24
25 because 4-cyanophenol does essentially not absorb at 380 nm, not even at 1 M concentration ($\epsilon_{380\text{nm}} \approx$
26
27 $0.03 \text{ M}^{-1} \text{ cm}^{-1}$; Figure S2). No correction for the impurity emission intensity at 542 nm was applied in
28
29 the case of the $[\text{Re}(\text{bpy})(\text{CO})_3(\text{pz})]^+$ data because the impurity emission is much weaker than that of the
30
31 rhenium complex.
32
33
34
35
36
37

38
39 The $[\text{Re}(\text{bpy})(\text{CO})_3(\text{pz})]^+$ luminescence lifetime decreases from 182 ns in the absence of 4-
40
41 cyanophenol to 24 ns in presence of ~1 M phenolic quencher (Figure 2b). The decay curves remain
42
43 single exponential up to 4-cyanophenol concentrations of 0.33 M and then become biexponential with a
44
45 slower decay component exhibiting a lifetime of ~200 ns. This observation may be a manifestation of
46
47 static quenching in phenol-rhenium adducts that are pre-associated before photoexcitation, but we note
48
49 that even at the highest phenol concentration the slow decay component contributes only 5 % to the total
50
51 emission decay. Consequently, the data analysis below will be based on the assumption of dynamic
52
53 emission quenching, as is customary when emission lifetimes and intensities are both dependent on the
54
55 quencher concentration.⁵²
56
57
58
59
60

Analogous luminescence quenching experiments were performed with deuterated 4-cyanophenol (CN-PhOD), and the results are shown in Figure 2c/2d. Even though the CN-PhOD concentrations in Figure 2c/2d were somewhat higher than those of CN-PhOH represented with equal colors in Figure 2a/2b, careful inspection of the data reveals that quenching is less pronounced when the phenol is in its deuterated form.

The magnitude of the H/D kinetic isotope effect (KIE) for $^3\text{MLCT}$ excited-state quenching of $[\text{Re}(\text{bpy})(\text{CO})_3(\text{pz})]^+$ by 4-cyanophenol can be estimated from the Stern-Volmer plots in Figure 2e/2f. The error bars associated with the individual data points arise essentially from the experimental uncertainty in determining relative emission intensities and luminescence lifetimes, which, from experience, is assumed to be 10%. From a linear regression fit to the emission intensity data (Figure 2e) a Stern-Volmer quenching constant ($K_{\text{SV}, \text{H}}$) of $4.2 \pm 0.2 \text{ M}^{-1}$ is obtained for CN-PhOH ($R^2 = 0.9856$) while $K_{\text{SV}, \text{D}} = 2.3 \pm 0.1 \text{ M}^{-1}$ for CN-PhOD ($R^2 = 0.9980$).⁵³ Given an inherent $^3\text{MLCT}$ lifetime (τ_0) of 182 ns for the $[\text{Re}(\text{bpy})(\text{CO})_3(\text{pz})]^+$ complex in aerated CH_3CN , one finds bimolecular quenching constants of $k_{\text{Q}, \text{H}} = (2.3 \pm 0.1) \cdot 10^7 \text{ M}^{-1} \text{ s}^{-1}$ and $k_{\text{Q}, \text{D}} = (1.3 \pm 0.1) \cdot 10^7 \text{ M}^{-1} \text{ s}^{-1}$ for undeuterated and deuterated 4-cyanophenol, respectively (Table 2). The ratio between $k_{\text{Q}, \text{H}}$ and $k_{\text{Q}, \text{D}}$ yields an H/D KIE of 1.8 ± 0.2 , suggesting that the rate-determining excited-state deactivation step involves proton motion.

Table 2. Stern-Volmer constants (K_{SV}), rate constants for bimolecular excited-state quenching (k_{Q}), and H/D kinetic isotope effects (KIE) for the two reaction couples as determined from emission intensities and lifetimes of the $[\text{Re}(\text{bpy})(\text{CO})_3(\text{pz})]^+$ (bpy/pz) or $[\text{Re}(\text{bpz})(\text{CO})_3(\text{py})]^+$ (bpz/py) complexes.

complex	exp. type	$K_{\text{SV}, \text{H}} [\text{M}^{-1}]$	$K_{\text{SV}, \text{D}} [\text{M}^{-1}]$	$k_{\text{Q}, \text{H}} [\text{M}^{-1} \text{ s}^{-1}]$	$k_{\text{Q}, \text{D}} [\text{M}^{-1} \text{ s}^{-1}]$	KIE
bpy/pz	intensity	4.2 ± 0.2	2.3 ± 0.1	$(2.3 \pm 0.1) \cdot 10^7$	$(1.3 \pm 0.1) \cdot 10^7$	1.8 ± 0.2
bpy/pz	lifetime	6.5 ± 0.2	3.7 ± 0.2	$(3.6 \pm 0.1) \cdot 10^7$	$(2.0 \pm 0.1) \cdot 10^7$	1.8 ± 0.2
bpz/py	intensity	1.02 ± 0.02	0.87 ± 0.03	$(3.3 \pm 0.1) \cdot 10^7$	$(2.8 \pm 0.1) \cdot 10^7$	1.2 ± 0.1
bpz/py	lifetime	0.63 ± 0.03	0.43 ± 0.03	$(2.0 \pm 0.1) \cdot 10^7$	$(1.4 \pm 0.1) \cdot 10^7$	1.4 ± 0.2

1
2 Stern-Volmer analysis of the emission lifetimes (Figure 2f) leads us to the same conclusion. The
3 Stern-Volmer constants in this case are $K_{SV, H} = 6.5 \pm 0.2 \text{ M}^{-1}$ ($R^2 = 0.9941$) and $K_{SV, D} = 3.7 \pm 0.2 \text{ M}^{-1}$ (R^2
4 $= 0.9838$), the bimolecular quenching constants are $k_{Q, H} = (3.6 \pm 0.1) \cdot 10^7 \text{ M}^{-1} \text{ s}^{-1}$ and $k_{Q, D} = (2.0 \pm 0.1) \cdot 10^7$
5 $\text{M}^{-1} \text{ s}^{-1}$ (Table 2). Thus, an H/D KIE of 1.8 ± 0.2 is found from the lifetime data, in agreement with the
6 value extracted from the emission intensities.
7
8
9
10
11
12

13
14
15
16 **[Re(bpz)(CO)₃(py)]⁺ luminescence quenching.** Analogous emission quenching experiments as
17 reported in the prior section were performed with the [Re(bpz)(CO)₃(py)]⁺ complex; the excitation
18 wavelength (λ_{exc}) in this case was 400 nm. The results are shown in Figure 3. An important difference to
19 the [Re(bpy)(CO)₃(pz)]⁺ complex is the comparatively short ³MLCT lifetime of [Re(bpz)(CO)₃(py)]⁺ (τ_0
20 $= 31 \text{ ns}$ in CH₃CN at 25°C), presumably the consequence of more efficient multiphonon relaxation from
21 the ³MLCT state which is lower in energy in the bpz complex than in the bpy complex.⁵⁴ The decrease
22 in ³MLCT energy also manifests in a red-shift of the emission band maximum ($\lambda_{max} \approx 644 \text{ nm}$)⁵⁵ relative
23 to that of [Re(bpy)(CO)₃(pz)]⁺ ($\lambda_{max} = 542 \text{ nm}$), and a weaker luminescence quantum yield. The
24 statement regarding quantum yields is made based on the observation of rhenium emission (between 550
25 nm and 750 nm) and impurity emissions (between 400 nm and 650 nm, see above) which are on the
26 same order of magnitude (Figure S3). In the spectra shown in Figure 3a/3c the impurity emission has
27 been subtracted (see the Supporting Information for details).
28
29
30
31
32
33
34
35
36
37
38
39
40
41
42
43
44
45
46
47
48
49
50
51
52
53
54
55
56
57
58
59
60

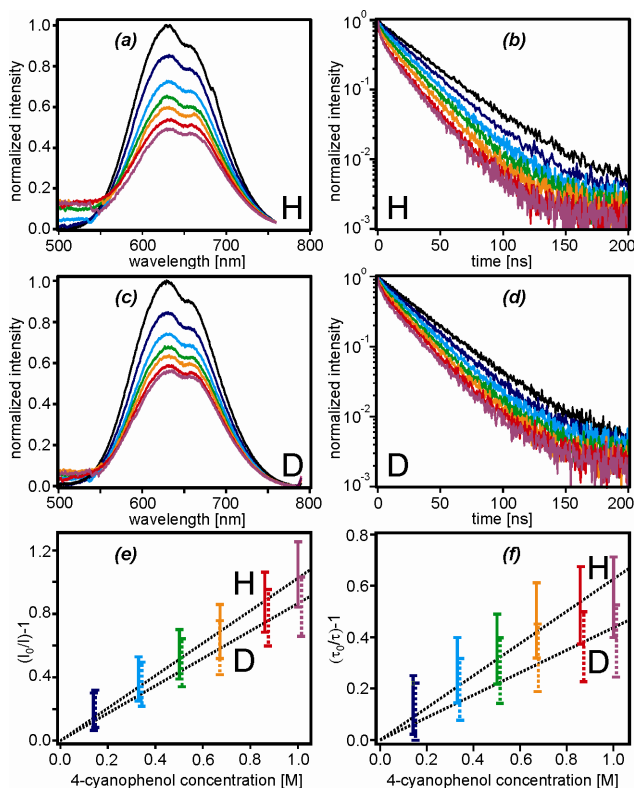


Figure 3. (a, c) Luminescence of $[\text{Re}(\text{bpz})(\text{CO})_3(\text{py})]^+$ in CH_3CN in presence of variable amounts of CN-PhOH (a) and CN-PhOD (c) after excitation at 400 nm. (b, d) Luminescence decays of the same complex detected at 630 nm under identical conditions following pulsed excitation at 340 nm. (e, f) Stern-Volmer plots based on the luminescence intensity (e) and lifetime (f) data. A consistent color code was used for all data; the concentrations used for the absorption and emission data in (a) – (d) can be read out from the Stern-Volmer plots in (e) and (f). The y-axes in (a) – (d) are in arbitrary units.

The luminescence decays detected at 630 nm also exhibit signs of impurity emission when 4-cyanophenol is added to a solution of $[\text{Re}(\text{bpz})(\text{CO})_3(\text{py})]^+$. Specifically, the decays are found to be tri-exponential even at moderate quencher concentrations. Measurements on CH_3CN solutions containing 4-cyanophenol but no rhenium show that two of the three decay components at 630 nm ($\tau_1 \approx 1.1$ ns and $\tau_2 \approx 4.5$ ns) are due to the emissive impurity (Figure S4). Consequently, only the slowest decay component ($\tau_3 > 10$ ns) is of interest in the luminescence quenching experiments from Figure 3b/3d.

1 Stern-Volmer analysis of the intensity and lifetime data in Figure 3a-3d results in the plots in Figure
2 3e/3f, and linear regression fits (R^2 values range from 0.9743 to 0.9985) yield Stern-Volmer constants
3 ($K_{SV, H}$, $K_{SV, D}$) and bimolecular excited-state quenching constants ($k_{Q, H}$, $k_{Q, D}$) as reported in Table 2.⁵⁶
4
5 The $k_{Q, H}$ and $k_{Q, D}$ values for $[\text{Re}(\text{bpz})(\text{CO})_3(\text{py})]^+$ turn out to be on the same order of magnitude as for
6
7 $[\text{Re}(\text{bpy})(\text{CO})_3(\text{pz})]^+$ (between $(1.4 \pm 0.1) \cdot 10^7 \text{ M}^{-1} \text{ s}^{-1}$ and $(3.3 \pm 0.1) \cdot 10^7 \text{ M}^{-1} \text{ s}^{-1}$); the luminescence
8
9 quenching observed in Figure 3a-3d is less pronounced than in Figure 2a-2d simply because
10
11 $[\text{Re}(\text{bpz})(\text{CO})_3(\text{py})]^+$ has a lower emission quantum yield and a shorter excited-state lifetime than
12
13 $[\text{Re}(\text{bpy})(\text{CO})_3(\text{pz})]^+$. Based on the $k_{Q, H}$ and $k_{Q, D}$ values for $[\text{Re}(\text{bpz})(\text{CO})_3(\text{py})]^+$ we obtain KIE =
14
15 1.2 ± 0.1 (from emission intensities) and 1.4 ± 0.2 (from lifetimes).
16
17
18
19
20
21
22
23

24 **Transient absorption spectroscopy.** In order to identify the photoproducts of the reaction between 4-
25 cyanophenol and the photoexcited rhenium complexes transient absorption spectroscopy is a useful
26
27 technique. Figure 4 shows the results from such experiments in which $\sim 10^{-5} \text{ M}$ solutions of
28
29 $[\text{Re}(\text{bpy})(\text{CO})_3(\text{pz})]^+$ (a), $[\text{Re}(\text{bpz})(\text{CO})_3(\text{py})]^+$ (b),⁵⁷ and $[\text{Re}(\text{bpy})(\text{CO})_3(\text{py})]^+$ (c) containing between 0
30
31 and $\sim 1 \text{ M}$ 4-cyanophenol were irradiated at 355 nm with laser pulses of $\sim 8 \text{ ns}$ duration; the spectra are
32
33 time-averaged over the first 200 ns after excitation. In the absence of quencher (black traces) an intense
34
35 and relatively narrow absorption band is observed for $[\text{Re}(\text{bpy})(\text{CO})_3(\text{pz})]^+$ (a) and $[\text{Re}(\text{bpy})(\text{CO})_3(\text{py})]^+$
36
37 (c) at 375 nm, while in $[\text{Re}(\text{bpz})(\text{CO})_3(\text{py})]^+$ (b) there is a weaker band at 370 nm. Based on prior
38
39 transient absorption studies of chemically closely related rhenium(I) tricarbonyl diimines the respective
40
41 bands are assigned to the reduced α -diimine ligand (bpy or bpz) of the $^3\text{MLCT}$ -excited
42
43 complexes.^{38,48,58-59}
44
45
46
47
48
49
50
51
52
53
54
55
56
57
58
59
60

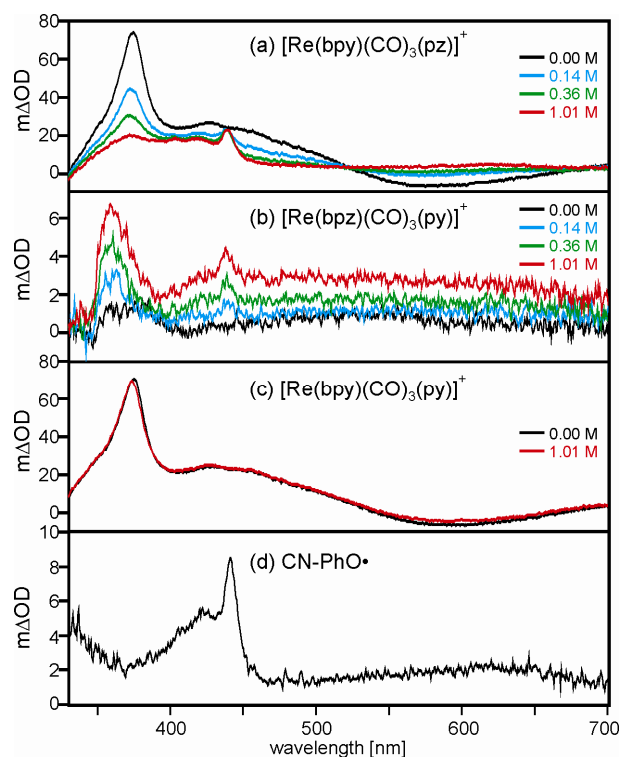


Figure 4. (a) Transient absorption spectra obtained from $\sim 10^{-5}$ M $[\text{Re}(\text{bpy})(\text{CO})_3(\text{pz})]^+$ solutions in CH_3CN in presence of variable concentrations of CN-PhOH (see inset). The data is time-averaged over 200 ns after excitation at 355 nm with ~ 8 ns pulses. An identical set of data is shown for the $[\text{Re}(\text{bpz})(\text{CO})_3(\text{py})]^+$ complex in (b) and for the $[\text{Re}(\text{bpy})(\text{CO})_3(\text{py})]^+$ reference complex in (c). (d) Transient absorption spectrum obtained from a $\sim 10^{-5}$ M solution of 4-cyanophenol in a 1:1 (v:v) mixture of CH_3CN and di-*tert*-butyl peroxide after excitation at 355 nm with ~ 8 ns pulses.

Upon addition of 4-cyanophenol significant spectral changes occur in the transient absorption spectra of Figure 4a/4b, while the spectrum of the reference complex (Figure 4c) stays essentially unchanged even after adding ~ 1 M CN-PhOH. The latter observation shows that 4-cyanophenol is unable to quench the $^3\text{MLCT}$ excited-state of $[\text{Re}(\text{bpy})(\text{CO})_3(\text{py})]^+$, and this is corroborated by luminescence experiments (Figure S8 of the Supporting Information).

In the cases of the two complexes with protonatable ligands there is a relatively narrow absorption band at 440 nm which gains intensity with increasing 4-cyanophenol concentration. A prior study

1 reported that the 4-cyanophenoxy radical (CN-PhO \cdot) exhibits an absorption maximum at 443 nm.⁶⁰ In
2 order to test whether the 440-nm band observed in Figure 4a/4b could indeed be due to CN-PhO \cdot , we
3 dissolved 4-cyanophenol in a 1:1 (v:v) mixture of acetonitrile and di-*tert*-butyl peroxide,⁶¹ and recorded
4 the optical absorption spectrum after exciting the sample at 355 nm with laser pulses of ~8 ns duration.
5 The result of this experiment is shown in Figure 4d and demonstrates quite convincingly that the 440 nm
6 absorption (and the weaker sideband at 420 nm) is due to CN-PhO \cdot ; in fact the spectrum in Figure 4d is
7 quite typical for phenoxy radicals.⁶⁰⁻⁶³

8
9
10 The direct observation of 4-cyanophenoxy radical in transient absorption strongly suggests that PCET
11 chemistry occurs between 4-cyanophenol and the photoexcited [Re(bpy)(CO)₃(pz)]⁺ and
12 [Re(bpz)(CO)₃(py)]⁺ complexes, even though we cannot unambiguously identify protonated and reduced
13 rhenium products. Whether the CN-PhO \cdot species is formed through concerted proton-electron transfer
14 (CPET) or consecutive electron transfer (ET) and proton transfer (PT) steps (in whatever sequence)
15 cannot be determined from our transient absorption experiments, mainly because the temporal resolution
16 is too low.

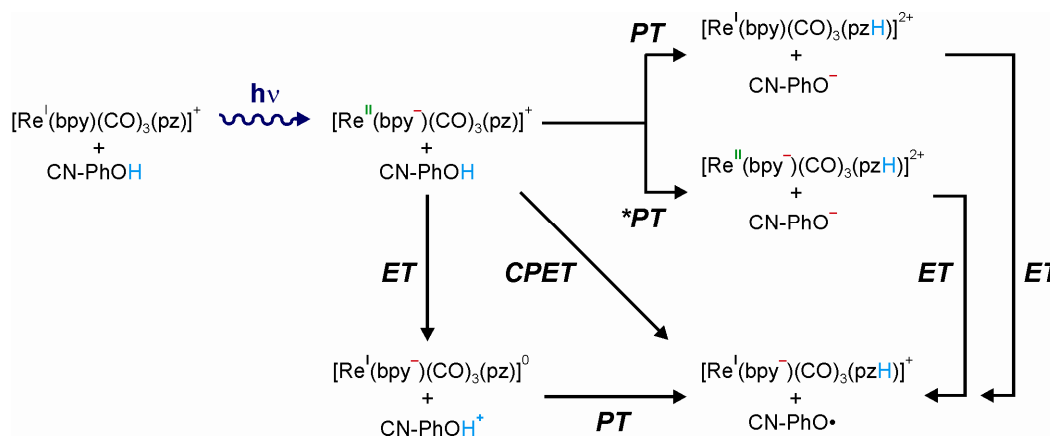
17
18
19 The photoproduction of phenoxy radicals implies the simultaneous formation of a rhenium reduction
20 product, either a [Re^I(bpy⁻)(CO)₃(pz)] (Figure 4a) or a [Re^I(bpz⁻)(CO)₃(py)] species (Figure 4b).⁸¹ The
21 respective species formally contain reduced bpy and bpz ligands, analogously to the ³MLCT-excited
22 forms of these complexes. Rhenium tricarbonyl diimines therefore usually exhibit similar transient
23 absorption spectra in their one-electron reduced forms and in their ³MLCT-excited forms,⁸² the signal
24 observed at ~375 nm in Figure 4a-c being the strongest absorption of bpy⁻ or bpz⁻. It appears that the
25 one-electron reduced form of [Re(bpy)(CO)₃(pz)]⁺ (red trace in Figure 4a) has a weaker extinction
26 coefficient at 375 nm than the ³MLCT-excited form of this complex (black trace in Figure 4a), but the
27 reasons for this observation are unclear. What seems clear, however, is that the 375-nm band is also
28 present in the spectrum of the [Re^I(bpy⁻)(CO)₃(pz)] species (red trace in Figure 4a); the phenoxy radical
29 absorption has a *minimum* at ~375 nm (Figure 4d) while there is clearly a local *maximum* near 375 nm in
30
31
32
33
34
35
36
37
38
39
40
41
42
43
44
45
46
47
48
49
50
51
52
53
54
55
56
57
58
59
60

the red spectrum of Figure 4a. Thus, there is direct evidence not only for a phenol oxidation product but also for a rhenium reduction product in all relevant cases.

Given the experimental uncertainty associated with the luminescence quenching experiments performed with $[\text{Re}(\text{bpz})(\text{CO})_3(\text{py})]^+$ (Figure 3) transient absorption studies would in principle be helpful to obtain complementary information about the reaction kinetics, but the temporal resolution of our transient absorption setup is insufficient for this purpose.

Driving-force and mechanistic considerations. Scheme 2 illustrates possible PCET reaction pathways for the 4-cyanophenol / $[\text{Re}(\text{bpy})(\text{CO})_3(\text{pz})]^+$ reaction couple. Aside from simple (radiative or nonradiative) relaxation to the ground state, four different deactivation processes are conceivable once the metal complex has been photoexcited: (i) photoinduced electron transfer followed by proton transfer (i. e., reaction along the lower left corner; ET, PT); (ii) photoinduced proton transfer to produce an excited deprotonated complex followed by electron transfer (*PT, ET); (iii) photoinduced proton transfer to produce deprotonated complex in its electronic ground state followed by electron transfer (PT, ET); (iv) concerted proton-electron transfer (CPET). Some thermodynamic considerations appear useful for elucidating which reaction pathways may be viable in our systems.^{6,17,64}

Scheme 2. Possible PCET reaction pathways.



The electrochemical properties of the $[\text{Re}(\text{bpz})(\text{CO})_3(\text{py})]^+$, $[\text{Re}(\text{bpy})(\text{CO})_3(\text{pz})]^+$, and $[\text{Re}(\text{bpy})(\text{CO})_3(\text{py})]^+$ complexes in acetonitrile have been previously investigated.^{34,45,47,50,65} Electrochemical potentials for one-electron reduction were generally reported versus the saturated calomel electrode, and in Table 3 we have converted the respective values to potentials (E_{red}) versus the ferrocenium/ferrocene (Fc^+/Fc) couple (by subtracting 0.38 V from the previously published values).⁶⁶ The reduction potentials of the $^3\text{MLCT}$ -excited complexes were estimated by adding the energy of the MLCT state (E_{MLCT}) to the ground-state reduction potentials, as is common practice.^{67, 68} From the last column in Table 3 we learn that the reduction potentials of the $^3\text{MLCT}$ -excited complexes are either around 1.0 V vs. Fc^+/Fc or below; the only exception is the dicationic $[\text{Re}(\text{bpy})(\text{CO})_3(\text{pz}-\text{CH}_3)]^{2+}$ complex having a methylated 1,4-pyrazine ligand which we will discuss later.

Table 3. Electrochemical potentials for one-electron reduction of the $[\text{Re}(\text{bpy})(\text{CO})_3(\text{pz})]^+$ (bpy/pz), $[\text{Re}(\text{bpz})(\text{CO})_3(\text{py})]^+$ (bpz/py), and $[\text{Re}(\text{bpy})(\text{CO})_3(\text{py})]^+$ (bpy/py) complexes in the electronic ground state (E_{red}) and in the $^3\text{MLCT}$ excited state (E_{red}^*) in Volts vs. Fc^+/Fc . E_{MLCT} is the energy of the $^3\text{MLCT}$ state.

complex	E_{red} [V]	E_{MLCT} [eV]	E_{red}^* [V]
bpy/pz	-1.59 ^b	2.26 ^f	0.67
bpz/py	-1.03 ^c	2.05 ^g	1.02
bpy/py	-1.49 ^d	2.26 ^h	0.77
bpy/pz- CH_3 ^a	-0.55 ^e	2.26 ^f	1.71

^a pz- CH_3 denotes a 1,4-pyrazine ligand which has been methylated at the peripheral N-atom, ^b from ref. 50, ^c from ref. 48, ^d from ref. 34, ^e from ref. 65, ^f estimated on the basis of E_{MLCT} in the bpy/pz complex and the reduction of the HOMO-LUMO energy gap between $[\text{Re}(\text{bpy})(\text{CO})_3(\text{pz})]^+$ and $[\text{Re}(\text{bpz})(\text{CO})_3(\text{py})]^+$, ^g from ref. 47, ^h assumed to be identical to the bpy/pz complex because $^3\text{MLCT}$ emission involves the same type of bpy ligand.

1 The electrochemical potential for one-electron oxidation of 4-cyanophenol (E_{ox}) has also been
2 reported previously.^{6,69-70} In acetonitrile solution, $E_{\text{ox}} = 1.40$ V vs. Fc^+/Fc for CN-PhOH .^{66,70}
3
4 Consequently, initial photoinduced electron transfer to any of the three monocationic rhenium
5 complexes of this study is thermodynamically improbable because this process is endergonic by ~ 0.4 eV
6
7 for $[\text{Re}(\text{bpz})(\text{CO})_3(\text{py})]^+$, ~ 0.6 eV for $[\text{Re}(\text{bpy})(\text{CO})_3(\text{py})]^+$, and ~ 0.7 eV for $[\text{Re}(\text{bpy})(\text{CO})_3(\text{pz})]^+$. What
8
9 is more, the comparatively large H/D KIE of 1.8 observed for $[\text{Re}(\text{bpy})(\text{CO})_3(\text{pz})]^+$ (see above) cannot
10
11 be reconciled with pure electron transfer in the rate-determining excited-state deactivation step.^{8-9,18}
12
13
14
15
16

17 Thermodynamic data for the proton transfer steps of Scheme 2 is experimentally difficult to access.
18
19 For ruthenium(II) complexes with protonatable bpz ligands acid-base titrations monitoring UV-vis
20
21 spectral changes can yield information about the pK_a values in the different redox states of the metal
22
23 center.⁷¹⁻⁷⁵ However, for our rhenium complexes the spectral changes occurring upon protonation are
24
25 minor, there appears to be simply no good (optical spectroscopic) handle for determination of the
26
27 ground-state pK_a values of $[\text{Re}(\text{bpz})(\text{CO})_3(\text{py})]^+$ and $[\text{Re}(\text{bpy})(\text{CO})_3(\text{pz})]^+$. However, it is possible to
28
29 determine the pK_a values of the $^3\text{MLCT}$ -excited $[\text{Re}(\text{bpz})(\text{CO})_3(\text{py})]^+$ and $[\text{Re}(\text{bpy})(\text{CO})_3(\text{pz})]^+$
30
31 complexes using luminescence spectroscopy (Figure S5/S6 of the Supporting Information). The
32
33 respective pK_a^* values are 3.4 ± 0.5 for $[\text{Re}(\text{bpy})(\text{CO})_3(\text{pz})]^+$ and 3.1 ± 0.5 for $[\text{Re}(\text{bpy})(\text{CO})_3(\text{pz})]^+$ in 1:1
34
35 (v:v) $\text{CH}_3\text{CN}/\text{H}_2\text{O}$ (Table S1 of the Supporting Information). 4-cyanophenol has a pK_a value of 9.0 ± 0.2
36
37 under identical experimental conditions (Figure S7). Thus, protonation of the photoexcited metal
38
39 complexes prior to electron transfer (*PT, ET sequence in Scheme 2) is thermodynamically unlikely.
40
41
42
43
44

45 However, we note that proton transfer coupled to electronic relaxation of the $^3\text{MLCT}$ -excited
46
47 complexes to their ground states (PT step in Scheme 2) is more exergonic by $\sim E_{\text{MLCT}}$ than proton
48
49 transfer to form rhenium complexes in their excited states (*PT step in Scheme 2), hence there may be
50
51 significant driving-force for the initial step of the PT, ET sequence of Scheme 2. However, based on the
52
53 (ground-state) reduction potential of the methylated $[\text{Re}(\text{bpy})(\text{CO})_3(\text{pz-CH}_3)]^{2+}$ complex (-0.55 V vs.
54
55 Fc^+/Fc ; Table 3), and an oxidation potential of 0.15 V vs. Fc^+/Fc for 4-cyanophenolate (in DMSO)^{6,69},
56
57 we estimate a reaction free energy of $+0.6$ eV for the ET step following the initial PT step in the 4-
58
59
60

1 cyanophenol / $[\text{Re}(\text{bpy})(\text{CO})_3(\text{pz})]^+$ reaction couple.⁷⁶ The highly endergonic nature of the subsequent
2 ET step should preclude the formation of PCET photoproducts as observed experimentally, at least in
3 the case of the $[\text{Re}(\text{bpy})(\text{CO})_3(\text{pz})]^+$ complex (Figure 4b). No electrochemical data for methylated or
4 the case of the $[\text{Re}(\text{bpy})(\text{CO})_3(\text{pz})]^+$ complex (Figure 4b). No electrochemical data for methylated or
5 protonated $[\text{Re}(\text{bpz})(\text{CO})_3(\text{py})]^+$ is available, but given the observation that $[\text{Re}(\text{bpz})(\text{CO})_3(\text{py})]^+$ is
6 easier to reduce than $[\text{Re}(\text{bpy})(\text{CO})_3(\text{pz})]^+$ by about 0.6 V (Table 3), the PT, ET sequence appears
7 thermodynamically more realistic in this case.
8
9
10
11
12

13
14 In short, from a thermodynamic perspective CPET appears as the most plausible PCET reaction
15 mechanism of the 4-cyanophenol / rhenium couples; for the $[\text{Re}(\text{bpz})(\text{CO})_3(\text{py})]^+$ complex the PT, ET
16 sequence cannot be fully excluded.
17
18
19
20
21
22
23
24
25
26
27

28 SUMMARY AND CONCLUSIONS

29
30
31
32

33 The rhenium complexes used in this study are less practical chromophores than previously
34 investigated $[\text{Ru}(\text{bpy})_2(\text{bpz})]^{2+}$ and $[\text{Ru}(\text{bpz})_3]^{2+}$ complexes because protonation effects are difficult to
35 detect by optical spectroscopic means. Nevertheless, transient absorption spectroscopy is able to provide
36 clear evidence for PCET chemistry because the spectral fingerprint of the 4-cyanophenoxy radical can
37 be detected. From a thermodynamics perspective, CPET appears as the most plausible reaction
38 mechanism for the 4-cyanophenol / $[\text{Re}(\text{bpy})(\text{CO})_3(\text{pz})]^+$ couple, and the experimentally observed H/D
39 KIE of 1.8 ± 0.2 is line with this expectation. CPET is thermodynamically viable also in the case of
40 $[\text{Re}(\text{bpz})(\text{CO})_3(\text{py})]^+$, but a PT, ET sequence (involving electronic relaxation in the PT step) cannot be
41 ruled out completely. A mixture of different mechanisms which are active at the same time cannot be
42 excluded either; only an ET, PT contribution can be ruled out safely based on thermodynamic grounds.
43
44 Thus, mechanistically the case has not become as clear as we had originally hoped, but the interesting
45 finding is that both rhenium complexes exhibit PCET chemistry with similar reaction rates even though
46
47
48
49
50
51
52
53
54
55
56
57
58
59
60

1 they have different excited-state structures in the sense that different sites become protonatable after
2 MLCT excitation. The bottom line is that for the reaction rates it does not appear to matter whether
3 MLCT excitation occurs towards the protonatable ligand or away from it, at least for the two reaction
4 couples investigated here.
5
6
7
8

14 EXPERIMENTAL SECTION

15
16
17
18
19 The rhenium(I) complexes were synthesized following previously published procedures,^{34,77} column
20 chromatography occurred on Silica Gel 60 from Machery-Nagel. Bruker Avance DRX 300 and B-ACS-
21 120 instruments were used for ¹H-NMR spectroscopy, electron ionization mass spectrometry (EI-MS)
22 was performed on a Finnigan MAT8200 instrument, for elemental analysis a Vario EL III CHNS
23 analyzer from Elementar was employed. Synthetic protocols and product characterization data are as
24 follows.
25
26
27
28
29
30
31

32
33 [Re(bpy)(CO)₃(pz)](PF₆). 500 mg (1.38 mmol) pentacarbonylchlororhenium(I) were suspended in 80
34 ml toluene along with 220 mg (1.41 mmol) 2,2'-bipyridine and heated to 110°C for 7 hours. After
35 cooling to room temperature the yellow Re(bpy)(CO)₃Cl precipitate (590 mg, 93%) was isolated by
36 suction filtration. Re(bpy)(CO)₃Cl was reacted with AgPF₆ (139 mg, 0.55 mmol) in 50 ml CH₃CN at
37 reflux for 13 hours. After cooling to room temperature the solution was filtered and the filtrate is
38 evaporated to yield [Re(bpy)(CO)₃(CH₃CN)](PF₆). The latter material was refluxed in 10 ml of a 3:10
39 (v:v) mixture of CH₂Cl₂ and CH₃OH along with 1,4-pyrazine (900 mg, 11.2 mmol) for 42 hours. The
40 hot solution was filtered, and the filtrate was evaporated to dryness. Purification of the raw product
41 occurred by column chromatography on silica gel using as an eluent first acetone, then a 10:1 (v:v)
42 mixture of acetone and H₂O, and finally a 100:10:1 (v:v:v) mixture of acetone, H₂O, and saturated
43 aqueous KNO₃ solution. Acetone was evaporated from the chromatography fractions containing the
44 desired complex, and precipitation of its hexafluorophosphate salt was induced by addition of saturated
45
46
47
48
49
50
51
52
53
54
55
56
57
58
59
60

aqueous KPF₆ solution. This procedure resulted in pure [Re(bpy)(pz)(CO)₃](PF₆) in 37% yield (41 mg).

¹H NMR (CD₃CN, 300MHz, 25°C): δ [ppm] = 7.82 (ddd, *J* = 7.6, 5.5, 1.5 Hz, 2H), 8.24 (dd, *J* = 3.0, 1.5 Hz, 2H), 8.30 (td, *J* = 7.9, 1.5 Hz, 2H), 8.42 (d, *J* = 8.1 Hz, 2H), 8.57 (dd, *J* = 3.0, 1.5 Hz, 2H), 9.22 (d, *J* = 5.5 Hz, 2H). ES-MS *m/z* = 507.0461 (calculated 507.0463 for C₁₇H₁₂N₄O₃Re⁺). Anal. calcd. for C₁₇H₁₂N₄O₃PF₆Re: C 31.34, H 1.86, N 8.60. Found: C 31.22, H 2.02, N 8.95.

[Re(bpy)(CO)₃(py)](CF₃SO₃). To [Re(bpy)(CO)₃(CH₃CN)](CF₃SO₃) which was available from prior studies^{43,78} in 26 ml of a 3:10 (v:v) mixture of CHCl₃ and CH₃OH was added pyridine (30 μL, 0.38 mmol), and the solution was refluxed under N₂ overnight. Subsequent column chromatography on silica gel using a 9:1 (v:v) mixture of CH₂Cl₂/CH₃OH afforded the pure product in 65% yield (148 mg). ¹H NMR (CDCl₃, 300MHz, 25°C): δ [ppm] = 7.45 – 7.35 (m, 2H), 7.74 (ddd, *J* = 7.6, 5.5, 1.3 Hz, 2H), 7.86 (tt, *J* = 7.6, 1.6 Hz, 1H), 8.22 – 8.14 (m, 2H), 8.37 (td, *J* = 8.0, 1.6 Hz, 2H), 8.89 (d, *J* = 8.2 Hz, 2H), 9.11 – 9.03 (m, 2H). ES-MS *m/z* = 506.0507 (calculated 506.0510 for C₁₈H₁₃N₃O₃Re⁺). Anal. calcd. for C₁₉H₁₃ N₃O₆F₃ReS: C 34.86, H 2.00, N 6.42. Found: C 34.88, H 1.96, N 6.40.

[Re(bpz)(CO)₃(py)](PF₆). Re(CO)₅Cl (330 mg, 1.00 mmol) and bpz (193 mg, 1.22 mmol) were refluxed in dry toluene overnight. After cooling to room temperature, the resulting purple solid is filtered and washed with pentane to yield Re(bpz)(CO)₃Cl in 68% yield (320 mg). The latter complex was reflux overnight in 12 ml CH₃CN along with 40 mg (0.17 mmol) AgPF₆. After cooling to room temperature the reaction mixture was filtrated to remove AgCl, and the filtrate was evaporated to dryness. The resulting orange solid was used for the next step without further purification. Pyridine (20 μL, 0.25 mmol) was added to a suspension of [Re(bpz)(CO)₃(CH₃CN)](PF₆) (117 mg, 0.20 mmol) in 26 ml of a 3:10 (v:v) mixture of CHCl₃ and CH₃OH, and the reaction mixture was refluxed under N₂ for 15 hours before evaporating the solvent. Product purification occurred by column chromatography on silica gel using as an eluent first pure acetone, then a 10:1 (v:v) mixture of acetone and H₂O, and finally a 100:10:1 (v:v:v) mixture of acetone, H₂O, and saturated aqueous KNO₃. Acetone was evaporated from the chromatography fractions containing the desired complex, and precipitation of its hexafluorophosphate salt was induced by addition of saturated aqueous KPF₆ solution. This procedure

1 resulted in 47 mg of pure product (36% yield). ^1H NMR (acetone- d_6 , 300MHz, 25°C): δ [ppm] = 7.65 –
2 7.36 (m, 2H), 8.05 (tt, $J = 7.7, 1.5$ Hz, 1H), 8.67 (dt, $J = 5.0, 1.5$ Hz, 2H), 9.26 (d, $J = 3.1$ Hz, 2H), 9.62
3 (dd, $J = 3.1, 1.3$ Hz, 2H), 10.18 (d, $J = 1.3$ Hz, 2H). ES-MS $m/z = 508.0412$ (calculated 508.0415 for
4 $\text{C}_{16}\text{H}_{11}\text{N}_5\text{O}_3\text{Re}^+$). Anal. calcd. for $\text{C}_{16}\text{H}_{11}\text{N}_5\text{O}_3\text{F}_6\text{PRe}\cdot 0.6 \text{C}_3\text{H}_6\text{O}$: C 31.11, H 2.14, N 10.19. Found: C
5 31.18, H 2.01, N 10.39.
6
7
8
9

10 For deuteration, 4-cyanophenol was dissolved in methanol- d_4 (99.80 % D) and stirred for 1 hour under
11 N_2 at room temperature. The solvent was removed subsequently using a rotary evaporator, and the
12 operation was repeated a second time. This procedure resulted in isotope purity on the order of 99%.
13 Acetonitrile for spectroscopic investigations was freshly distilled from P_2O_5 . UV-vis spectroscopy was
14 performed on a Cary 300 instrument. Luminescence spectra and lifetimes were measured a Fluorolog-
15 322 spectrometer equipped with a TCSPC option (Fluorohub FL-1061PC) and a TBC-07C detector
16 from Hamamatsu. For the lifetime experiments excitation occurred at 340 nm using a NanoLed-340
17 unit. Transient absorption experiments were conducted on an LP920-KS spectrometer from Edingburgh
18 Instruments with a detection system comprised of an iCCD camera from Andor and an R928
19 photomultiplier. Excitation occurred with the frequency-tripled output from a Quantel Brilliant b laser.
20 All spectroscopy measurements occurred in aerated solution, the absorbance of the rhenium complexes
21 at the excitation wavelength was typically between 0.1 and 0.3. The pH measurements occurred using a
22 standard pH meter.
23
24
25
26
27
28
29
30
31
32
33
34
35
36
37
38
39
40
41

42 Single crystals of $[\text{Re}(\text{bpz})(\text{CO})_3(\text{py})]_2(\text{PF}_6)_2(\text{H}_2\text{O})((\text{CH}_3)_2\text{CO})$ and $[\text{Re}(\text{bpy})(\text{CO})_3(\text{pz})](\text{PF}_6)$ were
43 coated with Paratone N-oil and mounted on a fiber loop followed by data collection at 100 K. The
44 crystallographic data was collected with a Bruker APEX II diffractometer, equipped with a graphite
45 monochromator centered on the path of $\text{MoK}\alpha$ ($\lambda = 0.71073 \text{ \AA}$) radiation. The SAINT program was used
46 to integrate the data, which was thereafter corrected for absorption using SADABS.⁷⁹ The structure was
47 solved by direct methods and refined by least-square fits on F^2 in SHELX97.⁸⁰ All non-hydrogen atoms
48 were refined anisotropically by full-matrix least-squares (SHELXL-97). Hydrogen atoms were placed
49 using a riding model. Their positions were constrained relative to their parent atom using the appropriate
50
51
52
53
54
55
56
57
58
59
60

HFIX command in SHELXL-97. In $[\text{Re}(\text{bpy})(\text{CO})_3(\text{pz})]_2(\text{PF}_6)_2 \cdot (\text{H}_2\text{O}) \cdot ((\text{CH}_3)_2\text{CO})$, the lattice acetone molecule was found to be disordered on two equivalent positions. Hydrogen atoms on this disordered acetone molecule and on the lattice water molecule were not introduced. Table 4 contains the summary of the unit cell and structure refinement parameters. The CIF files can be found in the supporting information. The CCDC numbers of the two structures are 877478 and 877479.

Table 4. Single crystal X-Ray diffraction parameters for $[\text{Re}(\text{bpy})(\text{CO})_3(\text{pz})]_2(\text{PF}_6)_2 \cdot (\text{H}_2\text{O}) \cdot ((\text{CH}_3)_2\text{CO})$ and $[\text{Re}(\text{bpz})(\text{CO})_3(\text{py})](\text{PF}_6)$.

	$[\text{Re}(\text{bpz})(\text{CO})_3(\text{py})](\text{PF}_6)$	$[\text{Re}(\text{bpy})(\text{CO})_3(\text{pz})]_2(\text{PF}_6)_2 \cdot (\text{H}_2\text{O}) \cdot ((\text{CH}_3)_2\text{CO})$
Formula	$\text{C}_{16}\text{H}_{11}\text{F}_6\text{N}_5\text{O}_3\text{PRe}$	$\text{C}_{37}\text{H}_{24}\text{F}_{12}\text{N}_8\text{O}_8\text{P}_2\text{Re}_2$
MW (g/mol)	652.47	1379.05
T(K)	100(2)	100(2)
Crystal System	monoclinic	monoclinic
Space group	$C2/c$	$C2/c$
a (Å)	43.0640(13)	23.463(4)
b (Å)	9.7300(3)	9.4086(16)
c (Å)	20.6150(6)	21.361(3)
β (°)	114.571(2)	109.374(8)
volume (Å ³)	7855.8(4)	4448.5(13)
Z	16	4
D (g·cm ⁻³)	2.207	2.059
$\mu_{\text{MoK}\alpha}$ (mm ⁻¹)	6.356	5.620
F000	4960.0	2648.0
GoF	1.052	1.109
^a R ₁ ($I > 2 \sigma(I)$)	0.0351	0.0174
^b wR ₂ (all reflections)	0.0897	0.0402

1
2
3
4
5
6
7
8
9
10
11
12
13
14
15
16
17
18
19
20
21
22
23
24
25
26
27
28
29
30
31
32
33
34
35
36
37
38
39
40
41
42
43
44
45
46
47
48
49
50
51
52
53
54
55
56
57
58
59
60

$${}^aR_1 = \Sigma||F_0| - |F_C||/\Sigma|F_0|, \text{ and } {}^b wR_2 = [\Sigma w(F_0^2 - F_C^2)^2/\Sigma w(F_0^2)^2]^{1/2}, w=1/[\sigma^2(F_0^2) + (aP)^2 + bP] \text{ and } P=(F_0^2 + 2F_C^2)/3$$

ACKNOWLEDGMENT

The authors thank Dr. Pierre Dechambenoit (Université de Bordeaux) for X-ray data collection. Funding from the Deutsche Forschungsgemeinschaft (DFG) through grants number WE4815/1-1 and INST186/872-1 is gratefully acknowledged.

SUPPORTING INFORMATION PARAGRAPH

Absorption and emission data of a sample from the 4-cyanophenol substance used in this work. Luminescence raw data from $[\text{Re}(\text{bpz})(\text{CO})_3(\text{py})]^+$, details regarding determination of (excited-state) pK_a values. Crystallographic data (cif files). This material is available free of charge via the Internet at <http://pubs.acs.org>.

REFERENCES

- (1) Mayer, J. M.; Rhile, I. J.; Larsen, F. B.; Mader, E. A.; Markle, T. F.; DiPasquale, A. G. *Photosynth. Res.* **2006**, *87*, 3.
- (2) Meyer, T. J.; Huynh, M. H. V.; Thorp, H. H. *Angew. Chem. Int. Ed.* **2007**, *46*, 5284.
- (3) Hammarström, L.; Styring, S. *Energy Environ. Sci.* **2011**, *4*, 2379.
- (4) Ramirez, B. E.; Malmström, B. G.; Winkler, J. R.; Gray, H. B. *Proc. Natl. Acad. Sci. U. S. A.* **1995**, *92*, 11949.

- 1
2
3
4
5
6
7
8
9
10
11
12
13
14
15
16
17
18
19
20
21
22
23
24
25
26
27
28
29
30
31
32
33
34
35
36
37
38
39
40
41
42
43
44
45
46
47
48
49
50
51
52
53
54
55
56
57
58
59
60
- (5) Concepcion, J. J.; Jurss, J. W.; Brennaman, M. K.; Hoertz, P. G.; Patrocinio, A. O. T.; Iha, N. Y. M.; Templeton, J. L.; Meyer, T. J. *Acc. Chem. Res.* **2009**, *42*, 1954.
- (6) Warren, J. J.; Tronic, T. A.; Mayer, J. M. *Chem. Rev.* **2010**, *110*, 6961.
- (7) Dempsey, J. L.; Winkler, J. R.; Gray, H. B. *Chem. Rev.* **2010**, *110*, 7024.
- (8) Hammes-Schiffer, S. *Acc. Chem. Res.* **2009**, *42*, 1881.
- (9) Hammes-Schiffer, S.; Stuchebrukhov, A. A. *Chem. Rev.* **2010**, *110*, 6939.
- (10) Costentin, C.; Robert, M.; Savéant, J.-M. *Acc. Chem. Res.* **2010**, *43*, 1019.
- (11) Biczok, L.; Gupta, N.; Linschitz, H. *J. Am. Chem. Soc.* **1997**, *119*, 12601.
- (12) Fang, Y.; Liu, L.; Feng, Y.; Li, X. S.; Guo, Q. X. *J. Phys. Chem. A* **2002**, *106*, 4669.
- (13) Cape, J. L.; Bowman, M. K.; Kramer, D. M. *J. Am. Chem. Soc.* **2005**, *127*, 4208.
- (14) Markle, T. F.; Rhile, I. J.; DiPasquale, A. G.; Mayer, J. M. *Proc. Natl. Acad. Sci. U. S. A.* **2008**, *105*, 8185.
- (15) Costentin, C.; Robert, M.; Savéant, J. M. *Phys. Chem. Chem. Phys.* **2010**, *12*, 11179.
- (16) Costentin, C.; Robert, M.; Savéant, J. M.; Tard, C. *Phys. Chem. Chem. Phys.* **2011**, *13*, 5353.
- (17) Mayer, J. M. *Annu. Rev. Phys. Chem.* **2004**, *55*, 363.
- (18) Huynh, M. H. V.; Meyer, T. J. *Chem. Rev.* **2007**, *107*, 5004.
- (19) Benisvy, L.; Bittl, R.; Bothe, E.; Garner, C. D.; McMaster, J.; Ross, S.; Teutloff, C.; Neese, F. *Angew. Chem. Int. Ed.* **2005**, *44*, 5314.

- 1
2
3
4
5
6
7
8
9
10
11
12
13
14
15
16
17
18
19
20
21
22
23
24
25
26
27
28
29
30
31
32
33
34
35
36
37
38
39
40
41
42
43
44
45
46
47
48
49
50
51
52
53
54
55
56
57
58
59
60
- (20) Sjödin, M.; Styring, S.; Åkermark, B.; Sun, L. C.; Hammarström, L. *J. Am. Chem. Soc.* **2000**, *122*, 3932.
- (21) Zhang, M.-T.; Irebo, T.; Johansson, O.; Hammarström, L. *J. Am. Chem. Soc.* **2011**, *133*, 13224.
- (22) Roberts, J. A.; Kirby, J. P.; Nocera, D. G. *J. Am. Chem. Soc.* **1995**, *117*, 8051.
- (23) Deng, Y. Q.; Roberts, J. A.; Peng, S. M.; Chang, C. K.; Nocera, D. G. *Angew. Chem. Int. Ed.* **1997**, *36*, 2124.
- (24) Roberts, J. A.; Kirby, J. P.; Wall, S. T.; Nocera, D. G. *Inorg. Chim. Acta* **1997**, *263*, 395.
- (25) Concepcion, J. J.; Brennaman, M. K.; Deyton, J. R.; Lebedeva, N. V.; Forbes, M. D. E.; Papanikolas, J. M.; Meyer, T. J. *J. Am. Chem. Soc.* **2007**, *129*, 6968.
- (26) Irebo, T.; Reece, S. Y.; Sjödin, M.; Nocera, D. G.; Hammarström, L. *J. Am. Chem. Soc.* **2007**, *129*, 15462.
- (27) Freys, J. C.; Bernardinelli, G.; Wenger, O. S. *Chem. Commun.* **2008**, 4267.
- (28) Gagliardi, C. J.; Westlake, B. C.; Kent, C. A.; Paul, J. J.; Papanikolas, J. M.; Meyer, T. J. *Coord. Chem. Rev.* **2010**, *254*, 2459.
- (29) Lebedeva, N. V.; Schmidt, R. D.; Concepcion, J. J.; Brennaman, M. K.; Stanton, I. N.; Therien, M. J.; Meyer, T. J.; Forbes, M. D. E. *J. Phys. Chem. A* **2011**, *115*, 3346.
- (30) Wenger, O. S. *Chem.-Eur. J.* **2011**, *17*, 11692.
- (31) Westlake, B. C.; Brennaman, M. K.; Concepcion, J. J.; Paul, J. J.; Bettis, S. E.; Hampton, S. D.; Miller, S. A.; Lebedeva, N. V.; Forbes, M. D. E.; Moran, A. M.; Meyer, T. J.; Papanikolas, J. M. *Proc. Natl. Acad. Sci. U. S. A.* **2011**, *108*, 8554.

- 1
2
3
4
5
6
7
8
9
10
11
12
13
14
15
16
17
18
19
20
21
22
23
24
25
26
27
28
29
30
31
32
33
34
35
36
37
38
39
40
41
42
43
44
45
46
47
48
49
50
51
52
53
54
55
56
57
58
59
60
- (32) Stewart, D. J.; Brennaman, M. K.; Bettis, S. E.; Wang, L.; Binstead, R. A.; Papanikolas, J. M.; Meyer, T. J. *J. Phys. Chem. Lett.* **2011**, *2*, 1844.
- (33) Bronner, C.; Wenger, O. S. *J. Phys. Chem. Lett.* **2012**, *3*, 70.
- (34) Sacksteder, L.; Zipp, A. P.; Brown, E. A.; Streich, J.; Demas, J. N.; DeGraff, B. A. *Inorg. Chem.* **1990**, *29*, 4335.
- (35) Wallace, L.; Rillema, D. P. *Inorg. Chem.* **1993**, *32*, 3836.
- (36) Sacksteder, L. A.; Lee, M.; Demas, J. N.; DeGraff, B. A. *J. Am. Chem. Soc.* **1993**, *115*, 8230.
- (37) Connick, W. B.; Di Bilio, A. J.; Hill, M. G.; Winkler, J. R.; Gray, H. B. *Inorg. Chim. Acta* **1995**, *240*, 169.
- (38) Chen, P. Y.; Westmoreland, T. D.; Danielson, E.; Schanze, K. S.; Anthon, D.; Neveux, P. E.; Meyer, T. J. *Inorg. Chem.* **1987**, *26*, 1116.
- (39) Schanze, K. S.; MacQueen, D. B.; Perkins, T. A.; Cabana, L. A. *Coord. Chem. Rev.* **1993**, *122*, 63.
- (40) Katz, N. E.; Mecklenburg, S. L.; Meyer, T. J. *Inorg. Chem.* **1995**, *34*, 1282.
- (41) Crane, B. R.; Di Bilio, A. J.; Winkler, J. R.; Gray, H. B. *J. Am. Chem. Soc.* **2001**, *123*, 11623.
- (42) Gabrielsson, A.; Hartl, F.; Zhang, H.; Smith, J. R. L.; Towrie, M.; Vlcek, A.; Perutz, R. N. *J. Am. Chem. Soc.* **2006**, *128*, 4253.
- (43) Hanss, D.; Walther, M. E.; Wenger, O. S. *Chem. Commun.* **2010**, *46*, 7034.

- 1
2
3
4
5
6
7
8
9
10
11
12
13
14
15
16
17
18
19
20
21
22
23
24
25
26
27
28
29
30
31
32
33
34
35
36
37
38
39
40
41
42
43
44
45
46
47
48
49
50
51
52
53
54
55
56
57
58
59
60
- (44) Blanco-Rodríguez, A. M.; Towrie, M.; Sykora, J.; Záliš, S.; Vlček, A. *Inorg. Chem.* **2011**, *50*, 6122.
- (45) Kirgan, R.; Simpson, M.; Moore, C.; Day, J.; Bui, L.; Tanner, C.; Rillema, D. P. *Inorg. Chem.* **2007**, *46*, 6464.
- (46) Oshin, K.; Landis, A. M.; Smucker, B. W.; Eichhorn, D. M.; Rillema, D. P. *Acta Crystallographica Section E* **2004**, *60*, m1126.
- (47) Perkins, T. A.; Hauser, B. T.; Eyler, J. R.; Schanze, K. S. *J. Phys. Chem.* **1990**, *94*, 8745.
- (48) Duesing, R.; Tapolsky, G.; Meyer, T. J. *J. Am. Chem. Soc.* **1990**, *112*, 5378.
- (49) MacQueen, D. B.; Schanze, K. S. *J. Am. Chem. Soc.* **1991**, *113*, 7470.
- (50) Lin, R. G.; Fu, Y. G.; Brock, C. P.; Guarr, T. F. *Inorg. Chem.* **1992**, *31*, 4346.
- (51) CH₃CN was distilled over P₂O₅ prior to use in spectroscopic experiments. Note that even the highest quality CH₃CN may contain concentrations of H₂O on the order of 0.1 mM or higher.
- (52) Stern, O.; Volmer, M. *Physikalische Zeitschrift* **1919**, *20*, 183.
- (53) The linear regression fits were forced to have an intercept of 0.
- (54) Caspar, J. V.; Meyer, T. J. *J. Phys. Chem.* **1983**, *87*, 952.
- (55) The dip in the luminescence bands at 650 nm is an instrumental artifact.
- (56) As noted above, the fits were forced to intercepts of 0.
- (57) The signal to noise ratio in (b) is lower than in (a) because the bpz complex has a shorter excited-state lifetime.
- (58) Van Wallendael, S.; Rillema, D. P. *Coord. Chem. Rev.* **1991**, *111*, 297.

- 1
2
3
4
5
6
7
8
9
10
11
12
13
14
15
16
17
18
19
20
21
22
23
24
25
26
27
28
29
30
31
32
33
34
35
36
37
38
39
40
41
42
43
44
45
46
47
48
49
50
51
52
53
54
55
56
57
58
59
60
- (59) Westmoreland, T. D.; Schanze, K. S.; Neveux, P. E.; Danielson, E.; Sullivan, B. P.; Chen, P.; Meyer, T. J. *Inorg. Chem.* **1985**, *24*, 2596.
- (60) Das, P. K.; Encinas, M. V.; Steenken, S.; Scaiano, J. C. *J. Am. Chem. Soc.* **1981**, *103*, 4162.
- (61) Gadosy, T. A.; Shukla, D.; Johnston, L. J. *J. Phys. Chem. A* **1999**, *103*, 8834.
- (62) Brede, O.; Orthner, H.; Zubarev, V.; Hermann, R. *J. Phys. Chem.* **1996**, *100*, 7097.
- (63) Lind, J.; Shen, X.; Eriksen, T. E.; Merenyi, G. *J. Am. Chem. Soc.* **1990**, *112*, 479.
- (64) Mayer, J. M.; Rhile, I. J. *Biochim. Biophys. Acta* **2004**, *1655*, 51.
- (65) Berger, S.; Klein, A.; Kaim, W.; Fiedler, J. *Inorg. Chem.* **1998**, *37*, 5664.
- (66) Pavlishchuk, V. V.; Addison, A. W. *Inorg. Chim. Acta* **2000**, *298*, 97.
- (67) Roundhill, D. M. *Photochemistry and Photophysics of Metal Complexes*; Plenum Press: New York, 1994.
- (68) Although potential values with two digits are reported, we note that these numbers represent estimates that are usually accurate to ca. 0.1 V.
- (69) Bordwell, F. G.; Cheng, J. P. *J. Am. Chem. Soc.* **1991**, *113*, 1736.
- (70) Yamaji, M.; Oshima, J.; Hidaka, M. *Chem. Phys. Lett.* **2009**, *475*, 235.
- (71) D'Angelantonio, M.; Mulazzani, Q. G.; Venturi, M.; Ciano, M.; Hoffman, M. Z. *J. Phys. Chem.* **1991**, *95*, 5121.
- (72) Ruge, A.; Clark, C. D.; Hoffman, M. Z.; Rillema, D. P. *Inorg. Chim. Acta* **1998**, *279*, 200.
- (73) Sun, H.; Hoffman, M. Z. *J. Phys. Chem.* **1993**, *97*, 5014.

1 (74) Venturi, M.; Mulazzani, Q. G.; Ciano, M.; Hoffman, M. Z. *Inorg. Chem.* **1986**, 25, 4493.

2
3 (75) Anderson, P. A.; Anderson, R. F.; Furue, M.; Junk, P. C.; Keene, F. R.; Patterson, B. T.;
4
5
6 Yeomans, B. D. *Inorg. Chem.* **2000**, 39, 2721.

7
8
9 (76) We assume that methylation and protonation of the pyrazine ligand have similar effects
10
11 on the reduction potential of this rhenium complex.

12
13
14 (77) Sullivan, B. P.; Meyer, T. J. *J. Chem. Soc., Chem. Commun.* **1984**, 1244.

15
16
17 (78) Walther, M. E.; Grilj, J.; Hanss, D.; Vauthey, E.; Wenger, O. S. *Eur. J. Inorg. Chem.*
18
19
20 **2010**, 4843.

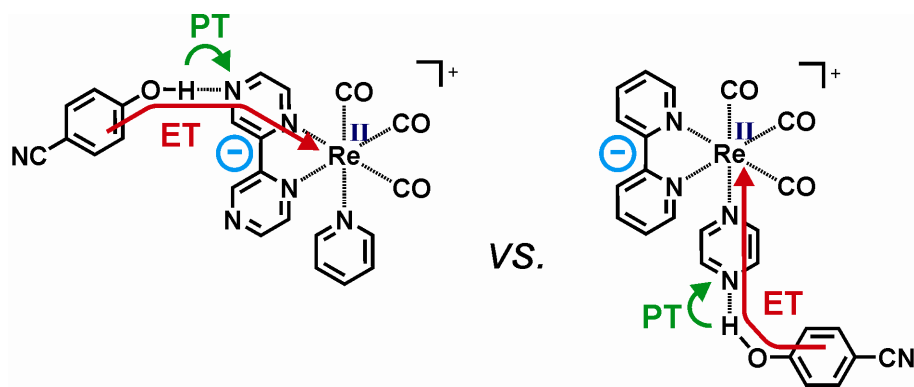
21
22
23 (79) Sheldrick, G. M. *SADABS, version 2.03; Bruker Analytical X-Ray Systems, Madison, WI*
24
25
26 **2000**.

27
28
29 (80) Sheldrick, G. M. *SHELXTL, Version 6.12; Bruker Analytical X-Ray Systems, Madison,*
30
31
32 *WI 2000*.

33
34 (81) To be more precise: The reduced *and protonated* forms, i. e., $[\text{Re}^{\text{I}}(\text{bpy}^-)(\text{CO})_3(\text{pzH})]^+$ and
35
36
37 $[\text{Re}^{\text{I}}(\text{bpzH})(\text{CO})_3(\text{py})]^+$.

38
39
40 (82) Záliš, S.; Cosani, C.; Cannizzo, A.; Chergui, M.; Hartl, F.; Vlček, A., Jr. *Inorg. Chim.*
41
42
43 *Acta* **2011**, 374, 578-585.

SYNOPSIS TOC



The influence of the directionality of MLCT excitation on photoinduced PCET between 4-cyanophenol and two closely related rhenium(I) complexes was investigated by luminescence and transient absorption spectroscopy. In one of the complexes MLCT excitation occurs towards a protonatable ligand, while in the other it occurs away from it. This difference in electronic excited-state structure appears to affect the mechanism of PCET but it has little influence on the PCET reaction rates.